ACS APPLIED MATERIALS & INTERFACES

www.acsami.org

Research Article

Hydrogel-Embedded Quantum Dot–Transcription Factor Sensors for Quantitative Progesterone Detection

Mingfu Chen, Chloé Grazon, Prerana Sensharma, Thuy T. Nguyen, Yunpeng Feng, Margaret Chern, R. C. Baer, Nitinun Varongchayakul, Katherine Cook, Sébastien Lecommandoux, Catherine M. Klapperich,* James E. Galagan,* Allison M. Dennis,* and Mark W. Grinstaff*

Cite This: *ACS Appl. Mater. Interfaces* 2020, 12, 43513–43521

Read Online

ACCESS | Metrics & More | Article Recommendations | Supporting Information

ABSTRACT: Immobilization of biosensors in or on a functional material is critical for subsequent device development and translation to wearable technology. Here, we present the development and assessment of an immobilized quantum dot–transcription factor–nucleic acid complex for progesterone detection as a first step toward such device integration. The sensor, composed of a polyhistidine-tagged transcription factor linked to a quantum dot and a fluorophore-modified cognate DNA, is embedded within a hydrogel as an immobilization matrix. The hydrogel is optically transparent, soft, and flexible as well as traps the quantum dot–transcription factor DNA assembly but allows free passage of the analyte, progesterone. Upon progesterone exposure, DNA dissociates from the quantum dot–transcription factor DNA assembly resulting in an attenuated ratiometric fluorescence output *via* Förster resonance energy transfer. The sensor performs in a dose-dependent manner with a limit of detection of 55 nM. Repeated analyte measurements are similarly successful. Our approach combines a systematically characterized hydrogel as an immobilization matrix and a transcription factor–DNA assembly as a recognition/transduction element, offering a promising framework for future biosensor devices.

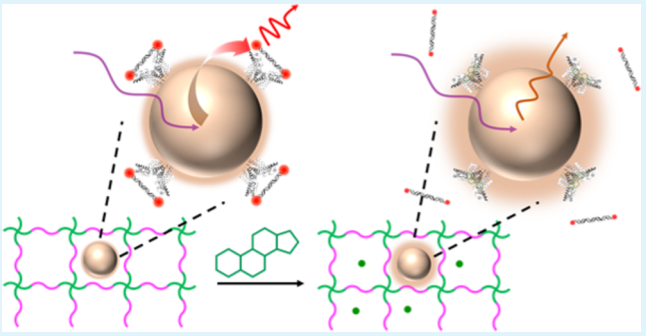

KEYWORDS: *biosensing, quantum dots, transcription factor, hydrogel, Förster resonance energy transfer*

1. INTRODUCTION

Digital health is positively transforming the life sciences from medical devices to diagnostics. Wearable sensor technologies will further drive the development of digital health and will provide a wealth of opportunities for detection and monitoring across the clinical landscape from cancer and trauma to addiction.[1] Yet, the full potential of digital health, and the subsequent benefit to patients, is not fully realized today because of the (1) limited number of antibodies, enzymes, and aptamers—*i.e.*, biorecognition elements—available for medical relevant biomarkers and (2) need for additional strategies to integrate biorecognition elements within sensors. With regard to sensor discovery, a recent genomics-to-sensor approach taps directly into the repertoire of natural bacterial regulatory circuits and identifies and harvests allosteric transcription factors (TF) for sensing. This new approach potentially addresses the problem of limited biosensors and expands the number and types of existing biorecognition elements.[2−4] Results from these metagenomic sequence mining approaches are yielding new TFs as biorecognition elements for (1) *in vivo* whole-cell sensors—*i.e.*, the bacterium itself is the biosensor[5−7] and (2) *in vitro* sensors—*i.e.*, the isolated bacterial TF is the sensing element in a biosensor.[8,9] In particular, our group has designed quantum dot-based Förster resonance energy transfer (FRET) nanosensors for progesterone, where progesterone binding alters TF–operator DNA affinity, affording a change in the proximity of the FRET donor (QD) and acceptor (fluorophore-labeled DNA) with subsequent fluorescence signal detection.[8]

Progesterone, a steroid hormone of significant clinical relevance, is the primary biomarker of reproductive status, and its monitoring in humans facilitates fertility planning and pregnancy.[10] Additionally, in cases of pregnancy of unknown location (PUL), progesterone is a validated biomarker of early gestation. Monitoring progesterone levels reduces the clinical burden of PUL cases and improves outcomes.[11,12] Measuring progesterone is also important in the livestock industry. For example, tracking the ovulation cycles of dairy cows and

Received: July 27, 2020
Accepted: September 7, 2020
Published: September 7, 2020

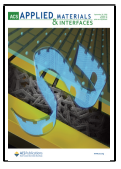

https://dx.doi.org/10.1021/acsami.0c13489
ACS Appl. Mater. Interfaces 2020, 12, 43513–43521

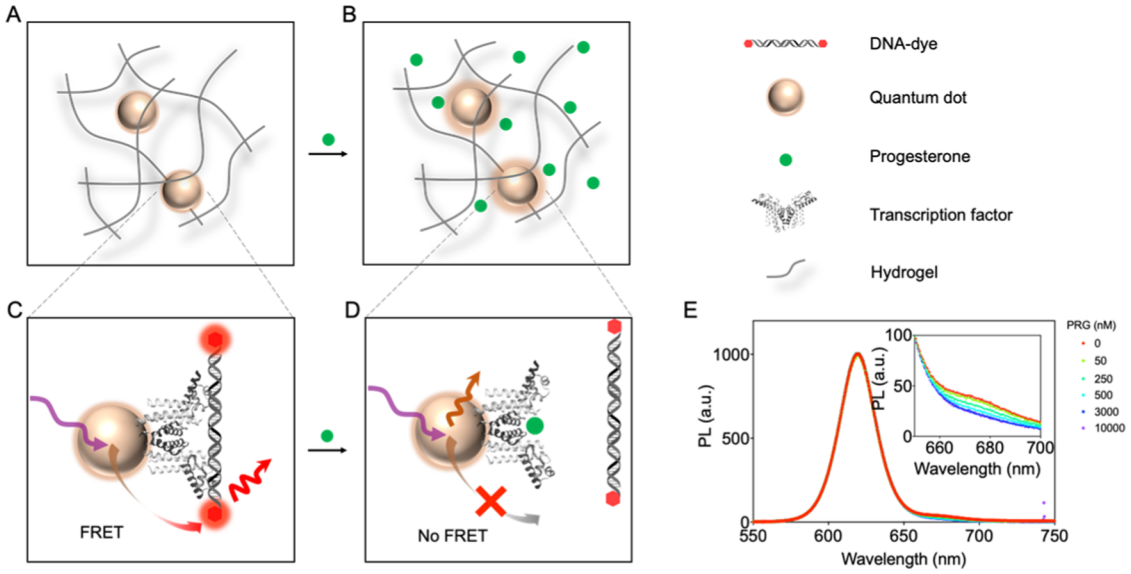

Figure 1. QD-based FRET sensor immobilized in the hydrogel. (A, B) Schematic illustration of progesterone diffusion into the hydrogel. (C, D) FRET-based sensor utilizing the TF−DNA binding mechanism. When progesterone (PRG) binds to the TF, the affinity between the TF and DNA reduces. The resulting dissociation of the TF−DNA complex produces a decreased FRET signal. (E) Representative spectra of sensor response to progesterone. A selection of the analyte concentrations is plotted for visual clarity. A zoomed-in figure is shown in the inset.

detecting pregnancy for fertility management leads to considerable cost saving for dairy farms.[13] Currently, steroid hormones are quantified using high-performance liquid chromatography (HPLC) or antibody-based immunoassays, and these analytical methods are ill-suited for real-time monitoring, repeated measurements, multiple sensing, or decentralized testing.[14−17]

The second challenge is integration of the discovered biorecognition element(s) and transduction mechanism into a device, a necessary step toward eventual use. Previously, QDs have been entrapped in hydrogels for phenol and dopamine chemo/biosensing purposes.[18−20] Moreover, immobilization of the biorecognition elements or sensors enables working under flow conditions required for integration in lateral flow[21,22] or microfluidic devices.[23,24] Herein, we describe a QD-based FRET sensor for progesterone immobilized within a robust covalently cross-linked hydrogel matrix. Specifically, we adapted our previous solution-phase QD-based FRET sensor,[8] composed of a polyhistidine-tagged transcription factor (SRTF1) self-assembled on a QD surface and a Cy5-fluorophore-labeled cognate DNA sequence. Binding of the TF to its cognate DNA site in the absence of progesterone enables FRET between the QD and Cy5; the presence of progesterone induces unbinding of the TF from the DNA with subsequent loss of FRET, yielding a progesterone concentration-dependent change in the fluorescence signal.[8] To our knowledge, this is the first report describing the integration of a transcription factor-based FRET sensor into a hydrogel and its subsequent performance, a critical step toward device prototyping. Specifically, we report the (1) preparation and characterization of the PEG hydrogel immobilization matrix; (2) sensor assembly; (3) diffusion studies of sensor constituents in the hydrogel; (4) sensor performance; and (5) repeated progesterone measurements.

2. MATERIALS AND METHODS

Sterol responsive allosteric transcription factor (SRTF1-his$_6$) and CdSe/CdS/ZnS QDs were prepared according to a previously reported procedure.[8,25] The QDs were transferred into water using a ligand-exchange procedure. The QDs are stable in aqueous buffer, with a quantum yield of 27 ± 3%.[25] Cy5-labeled HPLC-purified oligonucleotides were purchased from Integrated DNA Technologies, Inc. (Coralville, IA). Specifically, the polyhistidine-tagged transcription factor was self-assembled onto the QD surface at an average ratio of TFs to QD of 1 to 4 through chelation-based binding. Oligonucleotides labeled with Cy5−DNA containing SRTF1-his$_6$ binding sites were combined with QD−TFs at a specified ratio of DNA to QD (QD:DNA = 1/18).[8,25] The QD emission spectrum overlaps with the Cy5−DNA excitation spectrum to enable FRET (Figure S9). The TF binding to oligonucleotides depends on hydrogen bonding and van der Waals interactions between TF−DNA-binding domains and specific bases on oligonucleotides, and this interaction is disrupted upon binding of an analyte—*e.g.*, progesterone—resulting in separation of TF from DNA.[26] Metrics of sensor performance include EC$_{50}$ and limit of detection (LOD) values. EC$_{50}$ is the concentration of analyte that gives a half-maximal response. The LOD is defined as the progesterone concentration yielding a signal greater than 3 times the pool standard deviations above background.

We synthesized poly(ethylene glycol)-based hydrogels following published procedures.[27−29] Briefly, we mixed 4-arm-PEG−NH$_2$ in 1× borate buffer at pH 8.6 with NHS−PEG−NHS, which contains *N*-hydroxysuccinimide functionalities, in phosphate-buffered saline (PBS 1×) at pH 7.4 to form an amide-bond-linked network in the presence or absence of the QD-based FRET sensor.

The sensor was dialyzed against progesterone (PRG) solution overnight (Figure 1A,B). In the presence of progesterone, the transcription factor unbinds its cognate DNA site (Figure 1C,D). The sensor was then dialyzed against HEPES overnight to remove progesterone for another measurement. This cycle was repeated. Fluorescence measurements were recorded between cycles of progesterone exposure and removal. Fluorescence spectra were measured on a Nanolog spectrofluorometer (HORIBA, Ltd., NJ), equipped with a plate reader. The fluorescence intensity was monitored from 550 to 750 nm (λ_{exc} = 400 nm) with a 450 nm long-pass filter before the emission detector (Figure 1E). The intensity was recorded in relative fluorescence units, with baseline correction according to the manufacturer's instruction.

https://dx.doi.org/10.1021/acsami.0c13489
ACS Appl. Mater. Interfaces 2020, 12, 43513−43521

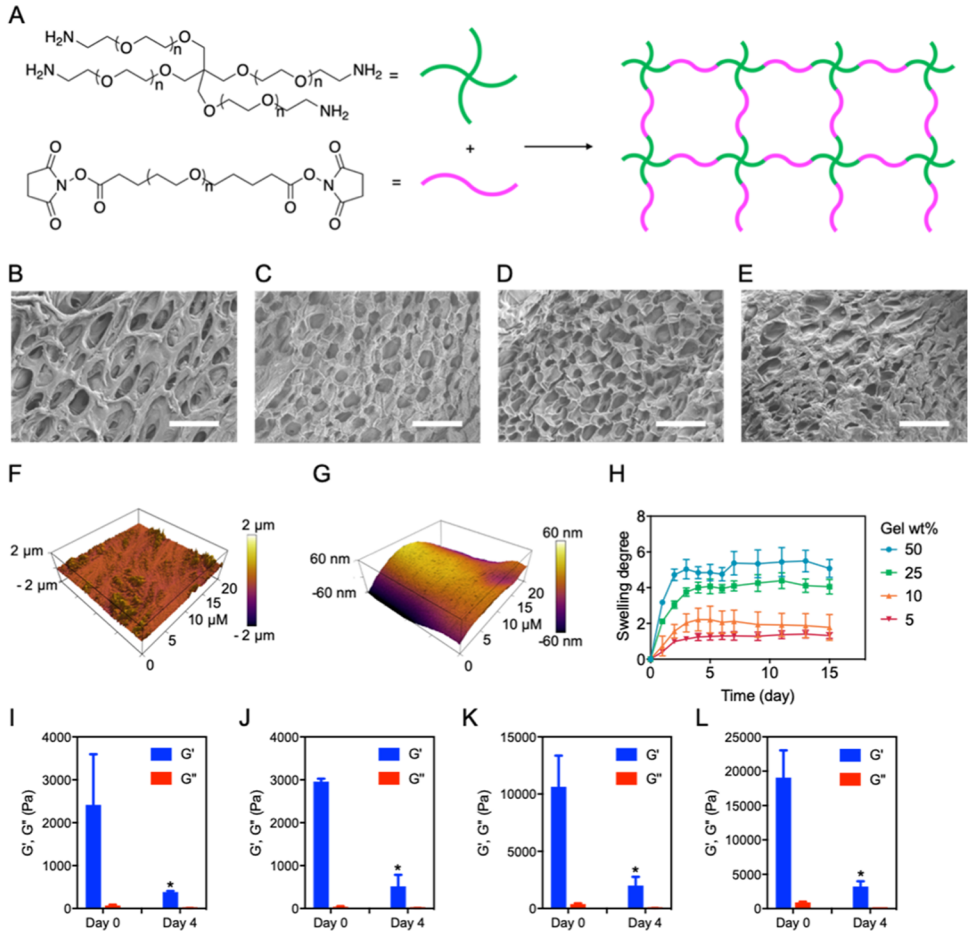

Figure 2. Hydrogel precursors, formation, and swelling. (A) Chemical structures of the hydrogel-forming components: 4-arm-PEG−NH_2 and NHS−PEG−NHS. Hydrogel formation proceeds *via* a reaction between the NHS ester and primary amine, producing a three-dimensional (3D) network. The cross-linked network enables encapsulation of the QD-based FRET sensor. Scanning electron microscopy images of (B) 5 wt %, (C) 10 wt %, (D) 25 wt %, and (E) 50 wt % hydrogels; scale bar is 50 μm. Atomic force microscopy (AFM) image of hydrogel (F) before and (G) after hydration. (H) Swelling degree of the hydrogel samples at 5, 10, 25, and 50 wt %, stored in PBS at 20 °C as a function of time. Storage and loss moduli of (I) 5 wt %, (J) 10 wt %, (K) 25 wt %, and (L) 50 wt % hydrogels with an oscillatory stress of 1 Pa at the frequency of 1 Hz before and after swelling. *Statistical significance (95% confidence) for mechanical strength relative to respective day 0 data.

All remaining experimental details, including characterization and assays, and statistical analysis are described in the Supporting Information.

3. RESULTS AND DISCUSSION

Solution-phase sensors have merits; however, integration of the design for analyte detection into the immobilization matrix expands the potential application space (*e.g.*, hydrogel electronics,[30] contact lens glucose sensor,[31,32] and hydrogel-based microsensors).[33] Additionally, successful incorporation of such sensors into lateral flow or microfluidic devices allows facile sample processing and precise flow control as well as integration with electronic devices for miniaturization.[34] As an initial step toward such devices, we recognize that our QD-based FRET sensors based on quantum dot-bound transcription factors and fluorophore-labeled nucleic acid duplexes are amenable to immobilization given the precedent for immobilized QDs in hydrogels for fluorescent probing and biocatalysis.[18,19] In the forthcoming text, we first describe the synthesis and characterization of the hydrogel, followed by the progesterone sensor construction and performance evaluation. Finally, we validate the performance of the sensor, by performing repeated measurements.

3.1. Hydrogel Synthesis and Characterization. We synthesized the poly(ethylene glycol)-based hydrogels following published procedures.[27,35,36] Specifically, we mixed 4-arm-PEG−NH_2 in borate buffer at pH 8.6 with NHS−PEG−NHS, which contains NHS esters, in phosphate-buffered saline (PBS 1×) at pH 7.4 to form the amide-bond-linked network (Figure 2A). We maintained the molar ratio of amine to NHS at 1:1 and varied the total concentration of the polymer in solution from 5 to 50 wt %.

First, we evaluated the pore size of the lyophilized hydrogels through scanning electron microscopy. Pore sizes are 14.4 ± 1.7, 11.8 ± 1.0, 10.3 ± 1.4, and 9.7 ± 0.4 μm for the 5, 10, 25, and 50 wt % hydrogels, respectively (Figure 2B−E). The pore size slightly decreases with increasing polymer weight percent. Additionally, we examined the morphology of the dried and hydrated hydrogel samples using atomic force microscopy (AFM). AFM analysis of the dried hydrogel reveals a surface roughness of 131 ± 21 nm, defined by the root-mean-square value of the height (Figure 2F). Upon hydration, the hydrogel exhibits a more homogeneous and smoother surface, with a decreased surface roughness of 19 ± 7 nm (Figure 2G). Next, we assessed the swelling characteristics of the hydrogels prior to integration with the QD-based FRET sensor. After exposure

https://dx.doi.org/10.1021/acsami.0c13489
ACS Appl. Mater. Interfaces 2020, 12, 43513−43521

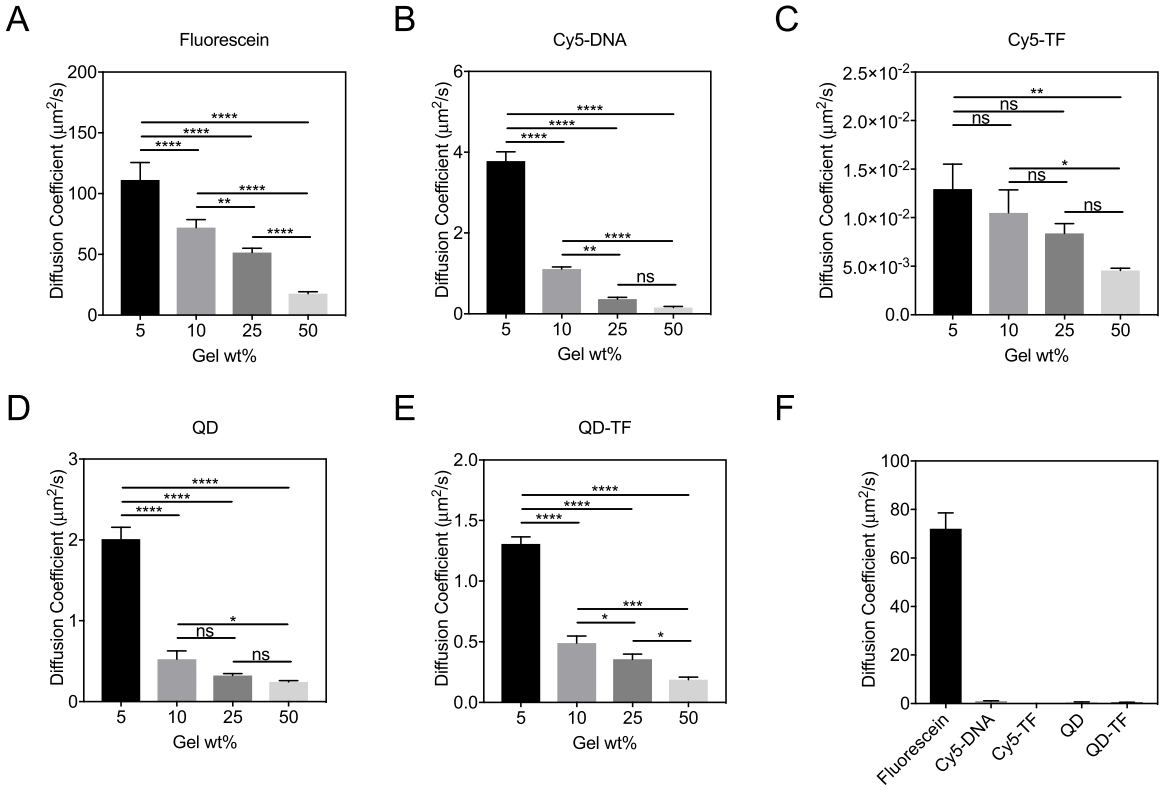

Figure 3. Diffusion coefficients of QD-based FRET sensor constituents. Diffusion coefficients of (A) fluorescein, (B) Cy5−DNA, and (C) Cy5−TF determined by fluorescence recovery after photobleaching (FRAP). Diffusion coefficients of (D) QD and (E) QD−TF determined by monitoring 100 nM QD or QD−TF diffusion into the hydrogel. (F) Diffusion coefficients of sensor constituents in the 10 wt % hydrogel. $N = 3$; $^{*}P \leq 0.05$; $^{**}P \leq 0.01$; $^{***}P \leq 0.001$; $^{****}P \leq 0.0001$; ns, not significant.

to PBS 1×, the hydrogels swell and reach equilibrium by day 4 for all polymer weight percent concentrations evaluated while maintaining their structural integrity (Figure 2H). The swelling degree positively correlates with the initial polymer content (percent by weight). The diffusion of small molecules (water, in this case) through the hydrogel translates to its capacity to absorb and release an analyte of interest, which is essential for biosensor functionality. As it is important that the hydrogels possess integrity, we evaluated the viscoelastic properties and mechanical strength of the hydrogels. First, we determined the linear viscoelastic region (LVR) by performing the oscillatory stress sweep (Figures S2, 3, 4, 5A). Next, we measured the frequency sweep at a controlled oscillatory stress of 1 Pa chosen from the LVR (Figures S2, 3, 4, 5C). Across the frequencies tested, the hydrogels exhibit solid-like behavior (*i.e.*, $G' > G''$). Lastly, we performed the same experiments on swelled hydrogels (Figures S2, 3, 4, 5B,D). The storage (G') and loss (G'') moduli positively correlate with the increase in weight percent of the hydrogels (Figure 2I−L). At the swelling equilibrium, the G' values decrease significantly for all four hydrogels compared to the as-prepared hydrogel prior to swelling. Taken together, the ability of the hydrogel to hold water translates to its capacity to absorb analyte solution and maintain an aqueous environment for the sensor components. For example, after exposure to PBS 1×, the 10 wt % hydrogel swells 221%, reaching equilibrium, while maintaining its integrity and mechanical strength to allow for use and easy handling. With tunable mechanical properties and structural integrity, these hydrogels hold promise for QD-based FRET sensor integration.

3.2. Diffusion Studies. The QD FRET sensor is based on an affinity-based biorecognition element.[8] This sensing framework requires binding of TF to its cognate DNA site in the absence of analytes and subsequent unbinding in the presence of analytes. As such, the immobilization matrix must successfully entrap the QD-based FRET (*i.e.*, quantum dot−transcription factor DNA assembly) sensor while allowing transport of the analyte and subsequent binding to the TF−DNA complex.

First, we characterized the diffusion of biomolecules within the hydrogels by fluorescence recovery after photobleaching (FRAP). Given a molecule's diffusion coefficient is affected by its molecular weight, we estimated the diffusion behavior of progesterone using fluorescein, a molecule with a similar molecular weight (fluorescein MW = 332.31 g/mol, progesterone MW = 314.46 g/mol). Fluorescein homogeneously distributes within the hydrogel and, upon photobleaching, within a region of interest, the fluorescence recovers as a function of time (Figure S6). The measured diffusion coefficient negatively correlates with hydrogel weight percent (Figure 3A). With increasing hydrogel weight percent, the mobility of fluorescein is statistically significantly hindered. We repeated the experiments with Cy5-labeled DNA and the fluorophore-labeled TF, SRTF1. Analogously, the Cy5-labeled DNA and SRTF1 exhibit decreasing diffusion coefficients with increasing hydrogel weight percent (descending correlation; Figure 3B,C). The entanglement and cross-linking of the hydrogel, which is tunable by varying the polymer weight percent, influences the diffusional coefficients of molecules and biomacromolecules, consistent with previous reports.[37−39]

https://dx.doi.org/10.1021/acsami.0c13489
ACS Appl. Mater. Interfaces 2020, 12, 43513−43521

Next, we measured the diffusion coefficients of QD and QD−TF under semi-infinite diffusion conditions. Unlike the experiments above, the QD is difficult to photobleach due to its photostability, rendering techniques like FRAP unsuitable for the diffusion coefficient measurements.[40] Thus, we directly monitored the mass transfer by acquiring vertical cross-sectional images of the hydrogel with the QD (or QD−TF) as it moved through the hydrogel (Figure S7). Fitting the intensity profiles of the cross-sectional images to Fick's second law yields the diffusion coefficient. The magnitude of the QD diffusion coefficient declines with respect to increasing hydrogel weight percent (Figure 3D). Conjugation of TF with QD further attenuates the diffusion coefficient of QD−TF (Figure 3E).

Lastly, we compared all of the diffusion coefficients of the species or sensor constituents in different wt % hydrogels. In the 5 wt % hydrogel, the small molecule fluorescein possesses a diffusion coefficient >25-fold higher than the other sensor constituents (Figure S8). In the 10 wt % hydrogel, the fluorescein possesses a diffusion coefficient >60-fold higher than the other sensor constituents (Figure 3F). Additionally, the absolute diffusion coefficients of fluorescein and the sensor constituents are decreased compared to the values measured in the 5 wt % hydrogel. The significantly faster diffusion of fluorescein indicates the feasibility of analyte molecules diffusing in and out of the hydrogel network, while the sensor components remain entrapped. In the 25 wt % hydrogel, the fluorescein possesses a diffusion coefficient >135-fold higher than the other sensor constituents, but the overall significantly hindered diffusion implies undesirable longer diffusion time to add or remove the analyte (to be described in Section 3.4). Collectively, these results suggest that the integration of QD-based FRET sensors into the hydrogel will (1) allow the progesterone molecules to diffuse in and out easily and (2) hinder the diffusion of the quantum dot−TF conjugate (FRET donor) and Cy5-fluorophore-modified DNA (FRET acceptor), thus minimizing the undesirable leakage of sensor constituents.[18,41] Consequently, we evaluated the 10 wt % hydrogels loaded with the QD-based FRET sensor throughout the course of the remaining studies.

3.3. Sensor Performance in Hydrogels. The discussion of the hydrogel-loaded QD-based FRET sensor is separated into three stages. First, we assembled the sensor constituents at a molar ratio of QD:TF:DNA = 1:4:18. Specifically, the FRET donor is the TF-conjugated QD, and the DNA oligonucleotide is decorated with fluorophores as the FRET acceptor. Next, we dissolved the two PEGylated macromonomers in the sensor solution and formed the hydrogel *in situ* to entrap sensors over approximately 30 min. When the TFs bind their cognate DNA binding sites in the absence of progesterone, the donors and acceptors are sufficiently close to enable energy transfer. Lastly, we exposed the QD-based FRET sensors embedded in the hydrogel to a solution of progesterone overnight. Upon progesterone binding to the transcription factor, the affinity of the TF for its cognate DNA reduces by several orders of magnitude;[8] the resultant unbinding of the TF and DNA increases the distance between the associated FRET donors and acceptors, producing a decrease in the fluorescence of the acceptor (F_A) and an increase in the fluorescence of the donor (F_D) (Figure S10). The sensor output is the normalized ratio of the integrated acceptor emission to the integrated donor emission (F_A/F_D). A four-parameter logistic function analysis of progesterone binding as a function of concentration reveals a dose-dependent decrease in sensor output (Figure 4). The constructed sensor permits the measurement of progesterone

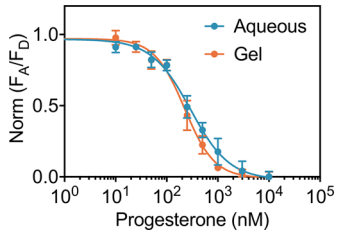

Figure 4. Dose−response curves for progesterone sensors in aqueous solution and in the 10 wt % hydrogel immobilization matrix, respectively. F_A/F_D at [PRG] = 0 nM is normalized to 1, F_A/F_D at [PRG] = 10 000 nM is normalized to 0, and linear interpolation is applied for concentrations in between.

from 78 to 632 nM. The EC_{50} and LOD values of the hydrogel-embedded sensor are 223 and 55 nM, respectively, and comparable to the solution-based counterpart (Table S2). This solution-based progesterone TF−DNA sensor does not respond to cholesterol, estrogen, 5β-pregnane-3α,20-α-diol, or 5β-pregnane-3α,20-α-diol-glucoronide while affords a 10 and 13% response to aldosterone and cortisol, respectively, indicating it is reasonably selective for progesterone.[8] Additionally, the progesterone TF−DNA sensor performs in artificial urine.[8]

Previously, QDs have been extensively employed in the context of solution-based sensors;[42−45] however, only recently has it been reported that hydrogel-embedded QDs (semiconductor quantum dots,[20,46−52] carbon dots,[53] and graphene quantum dots)[54,55] elicit effective analytical responses, similar to the results obtained herein. In addition, several studies report the successful integration of solution-based and QD-based sensors into microfluidic lab-on-a-chip systems[56,57] or microcapsules,[58] supporting the continued development of these types of sensors for real-world applications.

3.4. Repeated Progesterone Sensing. One can envision two sensing formats for a progesterone-measuring device: single or repeated use. The latter is more demanding from a device development standpoint as repeated use requires the TF/DNA complex to remain in close proximity for assembly and disassembly, while the analyte must be able to diffuse in and out. To assess our system's capability to perform multiple measurements, we subjected hydrogel-embedded QD-based FRET sensors to cycles of progesterone exposure and removal between measurements. The sensor output—the change in FRET—is derived from deconvolved fluorescence spectra and was fit to a four-parameter logistic function as described in (Figure 5). After regeneration, the sensor displays a dose-dependent response with an EC_{50} of 159 nM and R^2 = 0.76, comparable to the first-time sensing (EC_{50} = 223 nM and R^2 = 0.98). Notably, the relatively small differences in the dose-dependent sensor response in the first and second measurements (not statistically significantly different for most cases) show the potential of transcription factor-based biosensors in repeated sensing applications without the need for additional procedures to reform the nucleic acid−transcription factor complex for subsequent sensing (Figure S11). Greater variability is observed between measurements after dialysis, and this is likely due to limitations in the ability of dialysis to completely remove progesterone. Finally, we note that the relatively long time for dialysis to remove progesterone is a

https://dx.doi.org/10.1021/acsami.0c13489
ACS Appl. Mater. Interfaces 2020, 12, 43513−43521

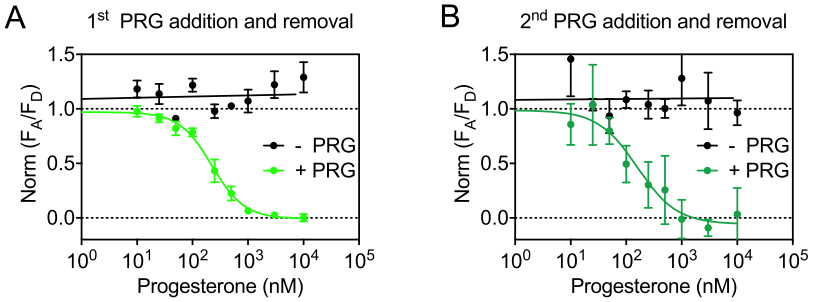

Figure 5. Reversibility of the progesterone sensor immobilized in the hydrogel. (A) Sensor response with the first cycle of progesterone (PRG) exposure and removal. (B) Sensor response with the second cycle of progesterone exposure and removal. With repeated cycles of progesterone exposure (+), dose−response curves are generated (green data points: light green points for the first PRG addition and dark green points for the second PRG addition). After PRG removal (−), sensor outputs are plotted at corresponding concentrations to which the same samples were exposed (black data points). With PRG addition, F_A/F_D at [PRG] = 0 nM is normalized to 1, F_A/F_D at [PRG] = 10 000 nM is normalized to 0, and linear interpolation is applied for concentrations in between. After PRG removal, F_A/F_D is scaled, where F_A/F_D at [PRG] = 0 nM is normalized to 1.

limitation for repeated measurements but not for single-use measurements, and this will need to be overcome in future designs.

The sensor consists of a transcription factor (SRTF1) linked to a core/shell/shell QD and a Cy5-fluorophore-labeled DNA, with an immobilization matrix composed of a hydrogel. From a sensor performance perspective, the LOD is 55 nM and the device is suitable for clinically relevant sample analysis.[59] Such a QD-based FRET sensor is also advantageous as it enables repeated analyte measurements. By contrast, immunoassays are considered effectively irreversible, stemming from fixation of antibody−analyte binding.[60] The regeneration of immunosensors poses significant barriers if prolonged use is desired.[61] As such, this study represents a first step toward assessing the potential of using transcription factor-based sensors in the context of single or repeated use for practical applications.

From a sensor design perspective, the potential versatility of our transcription factor-based sensor stems from diverse biorecognition elements mined from nature. In bacteria, TFs natively sense and react to a wide variety of stimuli and transduce a measurable transcriptional response—an alteration in reporter gene expressions.[62] Previously, TFs have been used as *in vivo* biosensors but are hampered by a slow response time and biosafety concerns for practical applications as the genetically reprogramed bacterium itself is the biosensor;[7,63−67] however, only recently has it been deployed *in vitro*, similar to this study.[68,69] The lack of characterized TFs for a wide variety of analytes prohibits the evaluation, optimization, and prototyping of next-generation biosensors. To address this problem, a recent genomics-to-sensor approach represents a potential paradigm shift in biosensor development, which identifies and harvests biosensing elements from high-throughput microbial genomic sequencing.[2,8] Metagenomic sequence mining continues to expand the repertoire of natural sensors[3,4] and tap directly into this rich diversity, being a first-line solution to the lack of biosensors. Finally, due to modular design of our sensor system, developing a family of new affinity-based FRET sensors becomes feasible, capitalizing on TFs with novel analyte specificities.

4. CONCLUSIONS

We describe a hydrogel-immobilized biosensor based on allosteric transcription factor−DNA binding. Specifically, this Förster resonance energy transfer sensor comprises a quantum dot−TF conjugate (FRET donor), a Cy5-fluorophore-modified DNA (FRET acceptor), and a hydrogel immobilization matrix. Upon progesterone binding, the QD−TF assembly dissociates, resulting in a decrease in ratiometric fluorescence output as the TF and QD are now no longer in close proximity. The key elements of this sensor include (1) TF−DNA coupling as a recognition/ transduction element; (2) fluorescent nanoparticles, QDs, that resist photobleaching and efficiently transfer energy to the fluorophore-labeled DNA; (3) a hydrogel immobilization matrix, polymerized *in situ* to entrap the sensors while enabling analyte diffusion and binding; (4) repeated progesterone sensing through capitalizing on the reversible interactions between the transcription factor and DNA. We foresee a convergence of high-throughput microbial genomic sequencing to identify new biorecognition elements and artificial intelligence algorithms to acquire and process sensor signals, as well as immobilization and integration into wearable microfluidic devices advancing digital health.

■ ASSOCIATED CONTENT

Supporting Information

The Supporting Information is available free of charge at https://pubs.acs.org/doi/10.1021/acsami.0c13489.

^{1}H NMR and ^{13}C NMR of 4-arm-PEG−NH_2 and NHS−PEG−NHS (Figure S1); mechanical properties of the 5% hydrogel (Figure S2); mechanical properties of the 10% hydrogel (Figure S3); mechanical properties of the 25% hydrogel (Figure S4); mechanical properties of the 50% hydrogel (Figure S5); diffusion coefficient measurement of fluorescein in the 10 wt % hydrogel (Figure S6); diffusion of QD in the 5% hydrogel (Figure S7); diffusion coefficients of the species or sensor constituents in different wt % hydrogels (Figure S8); absorption (dashed) and fluorescence emission (solid) of QDs (yellow, λ_{ex} = 400 nm) and Cy5−DNA (red, λ_{ex} = 590 nm) in the 10 wt % hydrogel (Figure S9); hydrogel-embedded sensor's response to analyte titration (Figure S10); reversibility of the sensor (Figure S11) (PDF)

■ AUTHOR INFORMATION

Corresponding Authors

Catherine M. Klapperich − *Department of Biomedical Engineering and Division of Materials Science and Engineering, Boston University, Boston, Massachusetts 02215, United States;*

https://dx.doi.org/10.1021/acsami.0c13489
ACS Appl. Mater. Interfaces 2020, 12, 43513−43521

Phone: 617-358-0253; Email: catherin@bu.edu; Fax: 617-353-6766

James E. Galagan − *Department of Biomedical Engineering and Department of Microbiology, Boston University, Boston, Massachusetts 02215, United States*; Phone: 617-358-0695; Email: jgalag@bu.edu

Allison M. Dennis − *Department of Biomedical Engineering and Division of Materials Science and Engineering, Boston University, Boston, Massachusetts 02215, United States*; orcid.org/0000-0001-5759-9905; Phone: 617-353-8509; Email: aldennis@bu.edu

Mark W. Grinstaff − *Department of Biomedical Engineering, Department of Chemistry, and Division of Materials Science and Engineering, Boston University, Boston, Massachusetts 02215, United States*; orcid.org/0000-0002-5453-3668; Phone: 617-358-3429; Email: mgrin@bu.edu; Fax: 617-353-6466

Authors

Mingfu Chen − *Department of Biomedical Engineering, Boston University, Boston, Massachusetts 02215, United States*

Chloé Grazon − *Department of Chemistry, Boston University, Boston, Massachusetts 02215, United States; CNRS, Bordeaux INP, LCPO, UMR 5629, Univ. Bordeaux, F-33600 Pessac, France*

Prerana Sensharma − *Department of Biomedical Engineering, Boston University, Boston, Massachusetts 02215, United States*

Thuy T. Nguyen − *Department of Biomedical Engineering, Boston University, Boston, Massachusetts 02215, United States*

Yunpeng Feng − *Department of Biomedical Engineering, Boston University, Boston, Massachusetts 02215, United States*

Margaret Chern − *Department of Biomedical Engineering, Boston University, Boston, Massachusetts 02215, United States*; orcid.org/0000-0003-3993-5500

R. C. Baer − *Department of Microbiology, Boston University, Boston, Massachusetts 02118, United States*

Nitinun Varongchayakul − *Department of Biomedical Engineering, Boston University, Boston, Massachusetts 02215, United States*

Katherine Cook − *Department of Chemistry, Boston University, Boston, Massachusetts 02215, United States*

Sébastien Lecommandoux − *CNRS, Bordeaux INP, LCPO, UMR 5629, Univ. Bordeaux, F-33600 Pessac, France*; orcid.org/0000-0003-0465-8603

Complete contact information is available at: https://pubs.acs.org/10.1021/acsami.0c13489

Author Contributions

M. Chen and M.W.G. conceptualized and designed the overall study. M. Chen conducted experiments and analyzed the data. C.G., T.T.N., and M. Chern assisted with QD preparation. P.S. helped collect spectral data. N.V. conducted AFM-related studies and analyzed the data. Y.F. assisted with diffusion measurement. R.C.B. provided the protein. K.C. analyzed NMR data. The manuscript was written by M. Chen and M.W.G. with contributions from all authors. All authors have given approval to the final version of the manuscript.

Notes

The authors declare the following competing financial interest(s): The authors have submitted a patent application on the biosensor technology.

ACKNOWLEDGMENTS

The authors recognize support and funding in part from NIH (U54EB015403, C.M.K.; CTSI 1KL2TR001411 and R01GM129437, A.M.D.), DARPA (W911NF-16-C-0044, J.E.G., M.W.G., C.M.K., A.M.D.), BU Kilachand (J.E.G.), BME distinguished fellowship (M. Chen), BUnano Terrier Tank award (M. Chen), Clare Booth Luce Graduate Fellowship (M. Chern), and Marie-Curie Fellowship from the European Union under the program H2020 (Grant 749973, C.G.). Research reported in this publication was supported by the Boston University Micro and Nano Imaging Facility, the Boston University Precision Diagnostics Center, and the Office of the Director, National Institutes of Health, under Award Number S10OD024993. The content is solely the responsibility of the authors and does not necessarily represent the official views of the funders.

REFERENCES

(1) Yetisen, A. K.; Martinez-Hurtado, J. L.; Ünal, B.; Khademhosseini, A.; Butt, H. Wearables in Medicine. *Adv. Mater.* **2018**, *30*, No. 1706910.

(2) Libis, V.; Delépine, B.; Faulon, J.-L. Sensing New Chemicals with Bacterial Transcription Factors. *Curr. Opin. Microbiol.* **2016**, *33*, 105−112.

(3) Rogers, J. K.; Taylor, N. D.; Church, G. M. Biosensor-Based Engineering of Biosynthetic Pathways. *Curr. Opin. Biotechnol.* **2016**, *42*, 84−91.

(4) Wan, X.; Marsafari, M.; Xu, P. Engineering Metabolite-Responsive Transcriptional Factors to Sense Small Molecules in Eukaryotes: Current State and Perspectives. *Microb. Cell Fact.* **2019**, *18*, 61.

(5) Zhang, J.; Jensen, M. K.; Keasling, J. D. Development of Biosensors and Their Application in Metabolic Engineering. *Curr. Opin. Chem. Biol.* **2015**, *28*, 1−8.

(6) Zhang, J.; Barajas, J. F.; Burdu, M.; Ruegg, T. L.; Dias, B.; Keasling, J. D. Development of a Transcription Factor-Based Lactam Biosensor. *ACS Synth. Biol.* **2017**, *6*, 439−445.

(7) Snoek, T.; Romero-Suarez, D.; Zhang, J.; Ambri, F.; Skjoedt, M. L.; Sudarsan, S.; Jensen, M. K.; Keasling, J. D. An Orthogonal and pH-Tunable Sensor-Selector for Muconic Acid Biosynthesis in Yeast. *ACS Synth. Biol.* **2018**, *7*, 995−1003.

(8) Grazon, C.; Baer, R. C.; Kuzmanović, U.; Nguyen, T.; Chen, M.; Zamani, M.; Chern, M.; Aquino, P.; Zhang, X.; Lecommandoux, S.; Fan, A.; Cabodi, M.; Klapperich, C.; Grinstaff, M. W.; Dennis, A. M.; Galagan, J. E.; Progesterone, A.; et al. Biosensor Derived from Microbial Screening. *Nat. Commun.* **2020**, *11*, No. 1276.

(9) Chen, M.; Nguyen, T. T.; Varongchayakul, N.; Grazon, C.; Chern, M.; Baer, R. C.; Lecommandoux, S.; Klapperich, C. M.; Galagan, J. E.; Dennis, A. M.; Grinstaff, M. W. Surface Immobilized Nucleic Acid−Transcription Factor Quantum Dots for Biosensing. *Adv. Healthcare Mater.* **2020**, No. 2000403.

(10) Posthuma-Trumpie, G. A.; van Amerongen, A.; Korf, J.; van Berkel, W. J. H. Perspectives for on-Site Monitoring of Progesterone. *Trends Biotechnol.* **2009**, *27*, 652−660.

(11) Memtsa, M.; Jurkovic, D.; Jauniaux, E. Diagnostic Biomarkers for Predicting Adverse Early Pregnancy Outcomes. *BJOG* **2019**, *126*, e107−e113.

(12) Pereira, P. P.; Cabar, F. R.; Gomez, ÚT.; Francisco, R. P. V. Pregnancy of Unknown Location. *Clinics* **2019**, *74*, No. e1111.

(13) Velasco-Garcia, M. N.; Mottram, T. Biosensors in the Livestock Industry: an Automated Ovulation Prediction System for Dairy Cows. *Trends Biotechnol.* **2001**, *19*, 433−434.

(14) Holst, J. P.; Soldin, O. P.; Guo, T.; Soldin, S. J. Steroid Hormones: Relevance and Measurement in the Clinical Laboratory. *Clin. Lab. Med.* **2004**, *24*, 105−118.

(15) Soldin, S. J.; Soldin, O. P. Steroid Hormone Analysis by Tandem Mass Spectrometry. *Clin. Chem.* **2009**, *55*, 1061−1066.

(16) Guedes-Alonso, R.; Montesdeoca-Esponda, S.; Sosa-Ferrera, Z.; Santana-Rodriguez, J. J. Liquid Chromatography Methodologies for the Determination of Steroid Hormones in Aquatic Environmental Systems. *Trends Environ. Anal. Chem.* **2014**, *3-4*, 14−27.
(17) D'Aurizio, F.; Cantu, M. Clinical Endocrinology and Hormones Quantitation: the Increasing Role of Mass Spectrometry. *Minerva Endocrinol.* **2018**, *43*, 261−284.
(18) Gattas-Asfura, K. M.; Zheng, Y.; Micic, M.; Snedaker, M. J.; Ji, X.; Sui, G.; Orbulescu, J.; Andreopoulos, F. M.; Pham, S. M.; Wang, C.; Leblanc, R. M. Immobilization of Quantum Dots in the Photo-Cross-Linked Poly(ethylene glycol)-Based Hydrogel. *J. Phys. Chem. B* **2003**, *107*, 10464−10469.
(19) Yuan, J.; Wen, D.; Gaponik, N.; Eychmüller, A. Enzyme-Encapsulating Quantum Dot Hydrogels and Xerogels as Biosensors: Multifunctional Platforms for Both Biocatalysis and Fluorescent Probing. *Angew. Chem., Int. Ed.* **2013**, *52*, 976−979.
(20) Jang, E.; Son, K. J.; Kim, B.; Koh, W.-G. Phenol Biosensor Based on Hydrogel Microarrays Entrapping Tyrosinase and Quantum Dots. *Analyst* **2010**, *135*, 2871−2878.
(21) Mahmoudi, T.; de la Guardia, M.; Shirdel, B.; Mokhtarzadeh, A.; Baradaran, B. Recent Advancements in Structural Improvements of Lateral Flow Assays towards Point-of-Care Testing. *TrAC, Trends Anal. Chem.* **2019**, *116*, 13−30.
(22) Posthuma-Trumpie, G. A.; Korf, J.; van Amerongen, A. Lateral Flow (Immuno)Assay: Its Strengths, Weaknesses, Opportunities and Threats. A Literature Survey. *Anal. Bioanal. Chem.* **2009**, *393*, 569−582.
(23) Liao, Z.; Zhang, Y.; Li, Y.; Miao, Y.; Gao, S.; Lin, F.; Deng, Y.; Geng, L. Microfluidic Chip Coupled with Optical Biosensors for Simultaneous Detection of Multiple Analytes: a Review. *Biosens. Bioelectron.* **2019**, *126*, 697−706.
(24) Brittain, W. J.; Brandstetter, T.; Prucker, O.; Rühe, J. The Surface Science of Microarray Generation−a Critical Inventory. *ACS Appl. Mater. Interfaces* **2019**, *11*, 39397−39409.
(25) Nguyen, T. T.; Chern, M.; Baer, R. C.; Galagan, J.; Dennis, A. M. A Förster Resonance Energy Transfer-Based Ratiometric Sensor with the Allosteric Transcription Factor TetR. *Small* **2020**, *16*, No. 1907522.
(26) Pabo, C. O.; Sauer, R. T. Transcription Factors: Structural Families and Principles of DNA Recognition. *Annu. Rev. Biochem.* **1992**, *61*, 1053−1095.
(27) Konieczynska, M. D.; Villa-Camacho, J. C.; Ghobril, C.; Perez-Viloria, M.; Tevis, K. M.; Blessing, W. A.; Nazarian, A.; Rodriguez, E. K.; Grinstaff, M. W. On-Demand Dissolution of a Dendritic Hydrogel-based Dressing for Second-Degree Burn Wounds through Thiol−Thioester Exchange Reaction. *Angew. Chem., Int. Ed.* **2016**, *55*, 9984−9987.
(28) Ghobril, C.; Rodriguez, E. K.; Nazarian, A.; Grinstaff, M. W. Recent Advances in Dendritic Macromonomers for Hydrogel Formation and Their Medical Applications. *Biomacromolecules* **2016**, *17*, 1235−1252.
(29) Konieczynska, M. D.; Villa-Camacho, J. C.; Ghobril, C.; Perez-Viloria, M.; Blessing, W. A.; Nazarian, A.; Rodriguez, E. K.; Grinstaff, M. W. A Hydrogel Sealant for the Treatment of Severe Hepatic and Aortic Trauma with a Dissolution Feature for Post-Emergent Care. *Mater. Horiz.* **2017**, *4*, 222−227.
(30) Lin, S.; Yuk, H.; Zhang, T.; Parada, G. A.; Koo, H.; Yu, C.; Zhao, X. Stretchable Hydrogel Electronics and Devices. *Adv. Mater.* **2016**, *28*, 4497−4505.
(31) Yao, H.; Shum, A. J.; Cowan, M.; Lähdesmäki, I.; Parviz, B. A. A Contact Lens with Embedded Sensor for Monitoring Tear Glucose Level. *Biosens. Bioelectron.* **2011**, *26*, 3290−3296.
(32) Yao, H.; Liao, Y.; Lingley, A. R.; Afanasiev, A.; Lähdesmäki, I.; Otis, B. P.; Parviz, B. A. A Contact Lens with Integrated Telecommunication Circuit and Sensors for Wireless and Continuous Tear Glucose Monitoring. *J. Micromech. Microeng.* **2012**, *22*, No. 075007.
(33) Peppas, N. A.; Van Blarcom, D. S. Hydrogel-Based Biosensors and Sensing Devices for Drug Delivery. *J. Controlled Release* **2016**, *240*, 142−150.
(34) Yan, J.; Pedrosa, V. A.; Simonian, A. L.; Revzin, A. Immobilizing Enzymes onto Electrode Arrays by Hydrogel Photolithography to Fabricate Multi-Analyte Electrochemical Biosensors. *ACS Appl. Mater. Interfaces* **2010**, *2*, 748−755.
(35) Gong, C.; Shan, M.; Li, B.; Wu, G. Injectable Dual Redox Responsive Diselenide-Containing Poly(Ethylene Glycol) Hydrogel. *J. Biomed. Mater. Res., Part A* **2017**, *105*, 2451−2460.
(36) Andrén, O. C. J.; Ingverud, T.; Hult, D.; Håkansson, J.; Bogestål, Y.; Caous, J. S.; Blom, K.; Zhang, Y.; Andersson, T.; Pedersen, E.; Björn, C.; Löwenhielm, P.; Malkoch, M. Antibiotic-Free Cationic Dendritic Hydrogels as Surgical-Site-Infection-Inhibiting Coatings. *Adv. Healthcare Mater.* **2019**, *8*, No. 1801619.
(37) Amsden, B. Solute Diffusion within Hydrogels. Mechanisms and Models. *Macromolecules* **1998**, *31*, 8382−8395.
(38) Weber, L. M.; Lopez, C. G.; Anseth, K. S. Effects of PEG Hydrogel Crosslinking Density on Protein Diffusion and Encapsulated Islet Survival and Function. *J. Biomed. Mater. Res. A* **2009**, *90*, 720−729.
(39) Waters, D. J.; Frank, C. W. Hindered Diffusion of Oligosaccharides in High Strength Poly(ethylene glycol)/Poly(acrylic acid) Interpenetrating Network Hydrogels: Hydrodynamic Versus Obstruction Models. *Polymer* **2009**, *50*, 6331−6339.
(40) Chern, M.; Kays, J. C.; Bhuckory, S.; Dennis, A. M. Sensing with Photoluminescent Semiconductor Quantum Dots. *Methods Appl. Fluoresc.* **2019**, *7*, No. 012005.
(41) Tavakoli, J.; Tang, Y. Hydrogel Based Sensors for Biomedical Applications: An Updated Review. *Polymers* **2017**, *9*, 364.
(42) Bagalkot, V.; Zhang, L.; Levy-Nissenbaum, E.; Jon, S.; Kantoff, P. W.; Langer, R.; Farokhzad, O. C. Quantum Dot−Aptamer Conjugates for Synchronous Cancer Imaging, Therapy, and Sensing of Drug Delivery Based on Bi-Fluorescence Resonance Energy Transfer. *Nano Lett.* **2007**, *7*, 3065−3070.
(43) Howes, P. D.; Chandrawati, R.; Stevens, M. M. Colloidal Nanoparticles as Advanced Biological Sensors. *Science* **2014**, *346*, No. 1247390.
(44) Wang, Y.; Howes, P. D.; Kim, E.; Spicer, C. D.; Thomas, M. R.; Lin, Y.; Crowder, S. W.; Pence, I. J.; Stevens, M. M. Duplex-Specific Nuclease-Amplified Detection of MicroRNA Using Compact Quantum Dot−DNA Conjugates. *ACS Appl. Mater. Interfaces* **2018**, *10*, 28290−28300.
(45) Wagner, A. M.; Knipe, J. M.; Orive, G.; Peppas, N. A. Quantum Dots in Biomedical Applications. *Acta Biomater.* **2019**, *94*, 44−63.
(46) Wu, W.; Aiello, M.; Zhou, T.; Berliner, A.; Banerjee, P.; Zhou, S. In-Situ Immobilization of Quantum Dots in Polysaccharide-Based Nanogels for Integration of Optical Ph-Sensing, Tumor Cell Imaging, and Drug Delivery. *Biomaterials* **2010**, *31*, 3023−3031.
(47) Wu, W.; Shen, J.; Banerjee, P.; Zhou, S. Chitosan-Based Responsive Hybrid Nanogels for Integration of Optical Ph-Sensing, Tumor Cell Imaging and Controlled Drug Delivery. *Biomaterials* **2010**, *31*, 8371−8381.
(48) Kim, J. H.; Lim, S. Y.; Nam, D. H.; Ryu, J.; Ku, S. H.; Park, C. B. Self-Assembled, Photoluminescent Peptide Hydrogel as a Versatile Platform for Enzyme-Based Optical Biosensors. *Biosens. Bioelectron.* **2011**, *26*, 1860−1865.
(49) Zhang, L.; Lei, J.; Liu, L.; Li, C.; Ju, H. Self-Assembled DNA Hydrogel as Switchable Material for Aptamer-Based Fluorescent Detection of Protein. *Anal. Chem.* **2013**, *85*, 11077−11082.
(50) Chen, L.; Tse, W. H.; Chen, Y.; McDonald, M. W.; Melling, J.; Zhang, J. Nanostructured Biosensor for Detecting Glucose in Tear by Applying Fluorescence Resonance Energy Transfer Quenching Mechanism. *Biosens. Bioelectron.* **2017**, *91*, 393−399.
(51) Cao, N.; Zhao, F.; Zeng, B. A Novel Self-Enhanced Electrochemiluminescence Sensor Based on PEI-Cds/Au@Sio2@ Ruds and Molecularly Imprinted Polymer for the Highly Sensitive Detection of Creatinine. *Sens. Actuators, B* **2020**, *306*, No. 127591.

https://dx.doi.org/10.1021/acsami.0c13489
ACS Appl. Mater. Interfaces 2020, 12, 43513−43521

(52) Qasemi, S.; Ghaemy, M. Highly Sensitive and Strongly Fluorescent Gum Tragacanth Based Superabsorbent Hydrogel as a New Biosensor for Glucose Optical Detection. *J. Mater. Chem. C* **2020**, *8*, 4148−4156.
(53) Cho, M.-J.; Park, S.-Y. Carbon-Dot-Based Ratiometric Fluorescence Glucose Biosensor. *Sens. Actuators, B* **2019**, *282*, 719−729.
(54) Ruiz-Palomero, C.; Benítez-Martínez, S.; Soriano, M. L.; Valcárcel, M. Fluorescent Nanocellulosic Hydrogels Based on Graphene Quantum Dots for Sensing Laccase. *Anal. Chim. Acta* **2017**, *974*, 93−99.
(55) Pincher, D. W. M.; Bader, C. A.; Hayball, J. D.; Plush, S. E.; Sweetman, M. J. Graphene Quantum Dot Embedded Hydrogel for Dissolved Iron Sensing. *ChemistrySelect* **2019**, *4*, 9640−9646.
(56) Jang, E.; Kim, S.; Koh, W.-G. Microfluidic Bioassay System Based on Microarrays of Hydrogel Sensing Elements Entrapping Quantum Dot−Enzyme Conjugates. *Biosens. Bioelectron.* **2012**, *31*, 529−536.
(57) Franke, M.; Leubner, S.; Dubavik, A.; George, A.; Savchenko, T.; Pini, C.; Frank, P.; Melnikau, D.; Rakovich, Y.; Gaponik, N.; Eychmüller, A.; Richter, A. Immobilization of pH-sensitive CdTe Quantum Dots in a Poly(acrylate) Hydrogel for Microfluidic Applications. *Nanoscale Res. Lett.* **2017**, *12*, No. 314.
(58) Xie, X.; Zhang, W.; Abbaspourrad, A.; Ahn, J.; Bader, A.; Bose, S.; Vegas, A.; Lin, J.; Tao, J.; Hang, T.; Lee, H.; Iverson, N.; Bisker, G.; Li, L.; Strano, M. S.; Weitz, D. A.; Anderson, D. G. Microfluidic Fabrication of Colloidal Nanomaterials-Encapsulated Microcapsules for Biomolecular Sensing. *Nano Lett.* **2017**, *17*, 2015−2020.
(59) Stanczyk, F. Z.; Gentzschein, E.; Ary, B. A.; Kojima, T.; Ziogas, A.; Lobo, R. A. Urinary Progesterone and Pregnanediol - Use for Monitoring Progesterone Treatment. *J. Reprod. Med.* **1997**, *42*, 216−222.
(60) Arugula, M. A.; Simonian, A. Novel Trends in Affinity Biosensors: Current Challenges and Perspectives. *Meas. Sci. Technol.* **2014**, *25*, No. 032001.
(61) Goode, J. A.; Rushworth, J. V. H.; Millner, P. A. Biosensor Regeneration: A Review of Common Techniques and Outcomes. *Langmuir* **2015**, *31*, 6267−6276.
(62) Lin, J.-L.; Wagner, J. M.; Alper, H. S. Enabling Tools for High-Throughput Detection of Metabolites: Metabolic Engineering and Directed Evolution Applications. *Biotechnol. Adv.* **2017**, *35*, 950−970.
(63) Fernandez-López, R.; Ruiz, R.; de la Cruz, F.; Moncalián, G. Transcription Factor-Based Biosensors Enlightened by the Analyte. *Front. Microbiol.* **2015**, *6*, No. 648.
(64) Mahr, R.; Frunzke, J. Transcription Factor-Based Biosensors in Biotechnology: Current State and Future Prospects. *Appl. Microbiol. Biotechnol.* **2016**, *100*, 79−90.
(65) Mimee, M.; Nadeau, P.; Hayward, A.; Carim, S.; Flanagan, S.; Jerger, L.; Collins, J.; McDonnell, S.; Swartwout, R.; Citorik, R. J.; Bulović, V.; Langer, R.; Traverso, G.; Chandrakasan, A. P.; Lu, T. K. An Ingestible Bacterial-Electronic System to Monitor Gastrointestinal Health. *Science* **2018**, *360*, 915−918.
(66) Skjoedt, M. L.; Snoek, T.; Kildegaard, K. R.; Arsovska, D.; Eichenberger, M.; Goedecke, T. J.; Rajkumar, A. S.; Zhang, J.; Kristensen, M.; Lehka, B. J.; Siedler, S.; Borodina, I.; Jensen, M. K.; Keasling, J. D. Engineering Prokaryotic Transcriptional Activators as Metabolite Biosensors in Yeast. *Nat. Chem. Biol.* **2016**, *12*, 951−958.
(67) Thompson, M. G.; Pearson, A. N.; Barajas, J. F.; Cruz-Morales, P.; Sedaghatian, N.; Costello, Z.; Garber, M. E.; Incha, M. R.; Valencia, L. E.; Baidoo, E. E. K.; Martin, H. G.; Mukhopadhyay, A.; Keasling, J. D. Identification, Characterization, and Application of a Highly Sensitive Lactam Biosensor from Pseudomonas putida. *ACS Synth. Biol.* **2020**, *9*, 53−62.
(68) de los Santos, E. L. C.; Meyerowitz, J. T.; Mayo, S. L.; Murray, R. M. Engineering Transcriptional Regulator Effector Specificity Using Computational Design and In Vitro Rapid Prototyping: Developing a Vanillin Sensor. *ACS Synth. Biol.* **2016**, *5*, 287−295.
(69) Li, S.; Zhou, L.; Yao, Y.; Fan, K.; Li, Z.; Zhang, L.; Wang, W.; Yang, K. A Platform for the Development of Novel Biosensors by Configuring Allosteric Transcription Factor Recognition with Amplified Luminescent Proximity Homogeneous Assays. *Chem. Commun.* **2017**, *53*, 99−102.

https://dx.doi.org/10.1021/acsami.0c13489
ACS Appl. Mater. Interfaces 2020, 12, 43513−43521